Memory of the unjamming transition during cyclic tiltings of a granular pile

S. Deboeuf,[1] O. Dauchot,[2] L. Staron,[3] A. Mangeney,[1] and J.-P. Vilotte[1]
[1]*Institut de Physique du Globe de Paris, Paris, France*
[2]*Service de Physique de l'État Condensé, CEA, Saclay, France*
[3]*Department of Applied Mathematics and Theoretical Physics, Cambridge, United Kingdom*
(Received 9 June 2005; published 28 November 2005)

Discrete numerical simulations are performed to study the evolution of the microstructure and the response of a granular packing during successive loading-unloading cycles, consisting of quasistatic rotations in the gravity field between opposite inclination angles. We show that internal variables—e.g., stress and fabric of the pile—exhibit hysteresis during these cycles due to the exploration of different metastable configurations. Interestingly, the hysteretic behavior of the pile strongly depends on the maximal inclination of the cycles, giving evidence of the irreversible modifications of the pile state occurring close to the unjamming transition. More specifically, we show that for cycles with maximal inclination larger than the repose angle, the weak-contact network carries the memory of the unjamming transition. These results demonstrate the relevance of a two-phase description—strong- and weak-contact networks—for a granular system, as soon as it has approached the unjamming transition.

DOI: 10.1103/PhysRevE.72.051305 PACS number(s): 45.70.−n, 83.80.Fg

I. INTRODUCTION

The discrete nature of granular materials makes their evolution very complex. In response to an external driving force, the macroscopic behavior of a granular system is determined by the intimate interplay between the evolving disordered microstructure—i.e., the arrangement of the grains and the geometry of their contact network—and the frictional interactions at the contacts, which allow for nontrivial force transmissions [1–3]. Even though significant advances have been made in the last decade [4–7], the underlying question of a physically based identification of the relevant internal variables and of their evolution laws remains open [8,9].

A particular issue of recent works on granular media concerns the transition from (to) a rigid-solid-like state to (from) a flowing-fluid-like state, due to its broad interest in geological and industrial processes and in particular to its challenge for condensed matter physics. This transition—e.g., the signature of the development of a yield stress or flow threshold in a disordered granular system or of an infinite relaxation time compared to the actual experimental time scale—has recently generated a flurry of activity [10–13]. Even though dense granular materials are athermal, it has recently been proposed that the transition could be seen as a "unjamming-jamming transition" at zero temperature [11,14,15], motivated by remarkable analogies between granular and glassy systems at both macroscopic and microscopic scales [16–19].

In this picture, the granular system is driven out of equilibrium under quasistatic external driving force, introducing fluctuations, as the system explores different packing configurations or metastable states that could be related to an "effective temperature" [20,21]. Important nonequilibrium effects of structurally disordered granular systems, beside the slow relaxation to equilibrium [12,22,23], are bistability and hysteresis [24–26] as the result of a memory effect due to the internal history dependence of systems out of equilibrium and the lack of a unique metastable state [2] and a jerky response to the external driving force with impulselike events (local rearrangements of grains or avalanches), as the result of the exploration of local minimal-energy configurations [27,28]. A related important question is whether a diverging length scale exists on the jammed side of the transition [29].

The well-known observation of different characteristic angles of the stability of granular systems results from such memory effects. When dense granular piles are inclined in the gravity field, there exists a maximal angle of stability, or avalanche angle θ_a at which the pile starts inevitably to flow, and an angle of repose $\theta_r < \theta_a$, defined as the slope angle at which the system comes back to rest. In the range $[\theta_r, \theta_a]$, the system exhibits a bistable behavior where it can be in a jammed—rigid—or an unjammed—flowing—state. In that region, the jammed state of the granular pile is conditionally stable; e.g., an avalanche can be triggered by perturbations of finite amplitude [30,31], evidencing metastability of the pile for slopes in $[\theta_r, \theta_a]$. Under rotation in the gravity field, the pile undergoes therefore a subcritical transition.

In [27,32,33], the unjamming transition of a two-dimensional (2D) cohesionless granular bed slowly tilted towards the avalanche angle θ_a was numerically investigated. This transition is characterized by a jerky response to the smooth rotation of the principal stress direction with respect to the packing, as attested by the occurrence of local rearrangements of grains. An analysis of the local stresses reveals the existence of a significant population of overloaded grains, carrying a shear stress ratio larger than the critical threshold of the packing at the unjamming transition. This allows one to define a coarse-graining length scale, or correlation length, which increases with the rotation up to an angle identified to θ_r, where it jumps to a length scale comparable with the thickness of the granular bed. This jump can be mapped onto a percolation transition of the overloaded grains and coincides with the onset of a packing dilation, indicating coherent shearing—a macroscopic shear strain

across the sample—prior to the unjamming transition. Further insights into the domain $[\theta_r, \theta_a]$ were achieved when analyzing the highly frictional contacts—e.g., the critical contacts where the friction is fully mobilized. Indeed the critical contacts are at incipient slip and likely give rise to local rearrangements of grains. A correlation length, based on the multiscale analysis of the critical contacts, exhibits a power-law-type divergence with an onset that coincides with θ_r. These highly frictional contacts tend to be associated with the weak-contact network, as defined in [34,35], suggesting a two-phase system and a second-order phase transition. The emergence of long-range "correlation lengths" within the range $[\theta_r, \theta_a]$, both in the stress and frictional states, is consistent with experimental measurements of both the amplitude of the local perturbation required to trigger an avalanche and the increasing scale of the response to a local perturbation, close to the unjamming transition [22,31]. This suggests that a peculiar regime exists before the unjamming transition—namely, in the range $[\theta_r, \theta_a]$, where the accumulation of frictional forces and resulting local rearrangements of grains leads to coherent shearing and enhances the structural disorder in the packing [36].

Such modifications of the microstructure of granular systems within the range $[\theta_r, \theta_a]$ at the unjamming transition should have a signature on nonequilibrium effects, such as the system hysteresis during cyclic solicitations. In contrast to cyclic shear solicitations [17,23,37–40], we focus here—in the continuation of [27,32,33]—on quasistatic cyclic rotations of dense cohesionless granular systems under gravity. Depending on the amplitude of the cyclic solicitations, the granular system can approach the unjamming transition, without overpass it, so as to keep a solidlike state and a quasistatic evolution. The internal history dependence or hysteresis can therefore be investigated depending on how far from equilibrium the system has been driven—i.e., on the distance from the unjamming transition. We report here results of discrete numerical simulations, based on the contact dynamics method, of quasistatic cyclic solicitations applied to a 2D cohesionless granular bed. These results show that the hysteresis does depend on the amplitude of the cycles and exhibit specific memory effects when the system approaches the unjamming transition, as a result of the structural evolution. In particular, the hysteresis is analyzed in terms of both strong- and weak-contact network contributions to the global response. It is found that the weak-contact network carries most of the signature of the memory effects, confirming the relevance of a two-phase description for the unjamming transition and extending it to the quasistatic rheology, as soon as the granular system has approached the transition.

The paper is organized as follows. The numerical procedure and details of the numerical simulations are presented in Sec. II. Section III focuses on critical contacts: after discussing previous results during monotonic external loading, we investigate the evolution of the critical contacts during relaxation and cyclic solicitations. In Sec. IV the hysteresis of the granular system is analyzed with respect to the amplitude of the cycles. Then the respective contributions of the weak- and strong-contact networks to the hysteresis of the packing are investigated in Sec. V. The paper ends with a discussion of the results in Sec. VI.

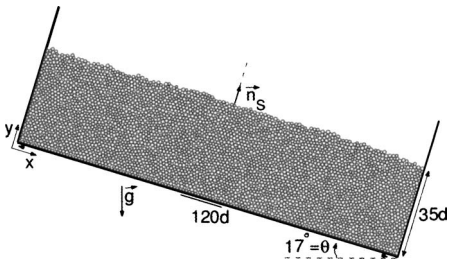

FIG. 1. A typical simulated granular pile of 4000 disks whose diameters are polydispersed at 20%, inclined at an angle $\theta=17°$ in the gravity field $\vec{g}$ with the xy frame linked to the bottom of the box and the unity vector normal to the free surface, $\vec{n}_S$.

II. NUMERICAL PROCEDURES

Discrete simulations of granular media take into account the individual existence of each grain constituting the system. The behavior of the collection of grains is entirely driven by the usual equations of motion and the contact laws ruling the interactions between the grains. The contact dynamics method, applied for this work, deals directly with infinitely stiff contact laws, assuming that grains interact through hard-core repulsion and nonsmooth Coulomb friction only [41]. This implies that the contact force between two grains is nonzero only if the latter are touching. Once a contact is created between two grains, the latter cannot get closer, so that any normal relative motion is only repulsive: the grains are perfectly rigid and cohesionless. The Coulomb frictional law consists of an inequality between the tangential and normal forces at contact, referred to as T and N, respectively: $\mp\mu N \leqslant T \leqslant \pm\mu N$, where μ is the microscopic coefficient of friction and sets a threshold for a contact to slip. Accordingly, this controls the frictional dissipation at the contact scale in the case $T=\pm\mu N$ when tangential slip motion is possible according to the immediate environment of the contact, by contrast with the case $\mp\mu N < T < \pm\mu N$, and no slip motion is allowed. In the present work, we are interested in the quasistatic evolution of the packing and concentrate on microplastic rearrangements only; therefore, we consider purely dissipative collisions and set the coefficient of restitution to zero.

The performed simulations are bidimensional. We consider packings of 4000 circular grains, randomly deposited in a rectangular box. The grains diameters are uniformly distributed in the interval $[d_{min}; d_{max}]$ with $d_{max}/d_{min}=1.5$. The polydispersity, measured as $(d_{max}-d_{min})/(2d)\simeq 20\%$ with d the mean disk diameter, prevents long-range crystal-like ordering in the packing by enhancing structural disorder. Each granular bed shows a nearly flat surface parallel to the bottom of the box, with a slope θ with respect to the horizontal direction; its thickness is $\simeq 35d$, and its length is $\simeq 120d$. The granular packings have an initial solid fraction $C\simeq 0.785$ and an initial coordination number $Z\simeq 3.46$. The microscopic coefficient of friction ($\mu=0.5$) is the same between all the grains and between the grains and the walls of the box. Figure 1 shows a typical granular pile inclined in the gravity field $\vec{g}$ at an angle $\theta=17°$, with the xy frame linked to the bottom of the box and the unity vector normal to the free

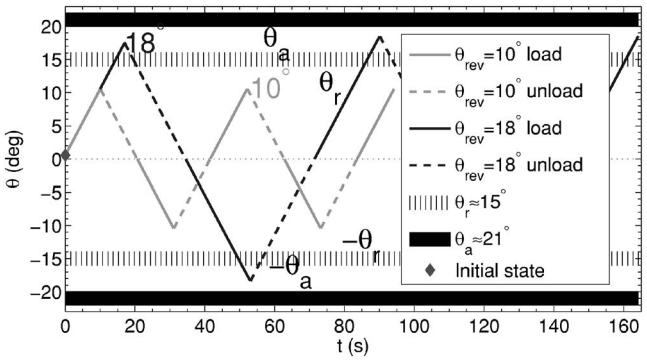

FIG. 2. Temporal plot of the surface slope $\theta(t)$ of the granular pile during the loading-unloading solicitations for $\theta_{rev}=10°$ (in gray) and $\theta_{rev}=18°$ (in black). The horizontal lines, with a thickness equal to the size of the fluctuations among 50 realizations, correspond to the repose and avalanche angles θ_r and θ_a. The initial state of the pile just before the cycles start is represented by a diamond.

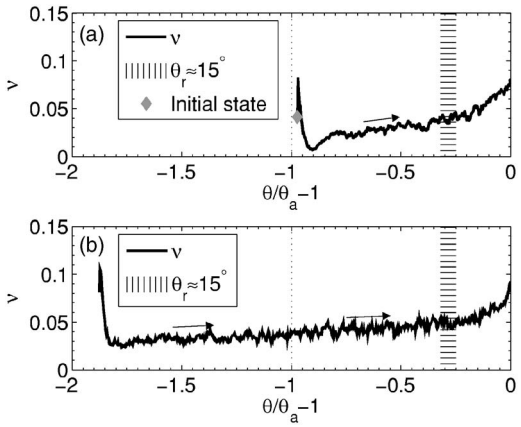

FIG. 3. Density of critical contacts ν averaged over 50 simulations (a) during the first loading starting from $\theta\simeq 0°$ and (b) during one large cycle, starting from a pile inclined at $-\theta_{rev}=-18°$, when varying the slope inclination towards the avalanche angle.

surface $\vec{n}_S$. In practice, instead of rotating the granular pile in the constant gravity field, the direction of $\vec{g}$ with respect to the pile is rotated to simulate tilting.

The cyclic solicitations consist of rotations at a constant rate (±0.001° per time step), the rotation being positive when clockwise. A positive rotation is first applied to newly generated granular piles so that the slope of the free surface increases from $\theta=0°$ to a maximal inclination angle θ_{rev}, corresponding to a loading stage. After the inclination θ_{rev} is reached, the direction of rotation is reversed and the slope decreases back to 0°, corresponding to an unloading stage. Rotation is maintained so that the slope of the pile evolves from 0 toward the opposite maximal inclination angle $-\theta_{rev}$. The direction of rotation is again reversed, and the cyclic solicitation is resumed. Two successive cycles are performed. This solicitation is applied on 50 granular piles differing in the initial disordered microstructure—i.e., the grain arrangement and the contact network geometry, showing characteristic angles $\theta_r\simeq 15°$ and $\theta_a\simeq 21°$. In the following, averages are taken over all 50 simulations. The granular beds and data describing the first loading stage are the actual data of Staron *et al.* [32].

We study the influence of the cycle amplitude and distance from the unjamming transition on the evolution of the pile state by considering two values of the maximal inclination angle θ_{rev}—namely, by applying small and large cycles. The smallest value of θ_{rev} is chosen so that the small cycle keeps the pile out of the coherent shear regime identified prior to the unjamming transition: $\theta_{rev}=10°<\theta_r$. On the contrary, the largest value of θ_{rev} is chosen in the range of slopes $[\theta_r;\theta_a]$, but below the minimal avalanche angle observed among the 50 realizations to prevent the pile from avalanching: $\theta_{rev}=18°\in[\theta_r;\theta_a]$. These two kinds of cycles are represented in Fig. 2, where the slope of the pile θ is plotted against the time t for both small (in gray) and large (in black) cycles. Solid lines represent loading stages, and dashed lines represent unloading ones. The horizontal lines indicate the repose and avalanche angles θ_r and θ_a, with a thickness equal to the size of the fluctuations. A diamond indicates the initial state of the granular pile just before the cycles start, which will be reported on all the next figures.

III. CRITICAL CONTACT CLUSTERING

As discussed in the case of slow monotonic external loading of a granular slope in [27,32,33], the coherent shear regime identified prior to the unjamming transition corresponds to the structuration in the packing of highly frictional contacts—e.g., contacts where forces have reached the Coulomb frictional threshold—i.e., $T=\pm\mu N$—referred to as critical contacts. An interesting issue would be the evolution of the critical contacts during cyclic solicitations.

We discuss first the robustness of previous results on critical contacts [27,33] against the pile preparation. Figure 3 displays the evolution of the density of critical contacts ν, defined as the proportion of critical contacts to the total number of contacts in a granular packing, averaged over 50 piles, when varying the pile inclination θ toward θ_a, from 0° (a) and from $-\theta_{rev}=-18°$ (b). At the beginning of the solicitation, both evolutions of ν show a sudden drop to a minimum value indicating the instantaneous loss of critical contacts. After this first stage and in spite of the different initial conditions, the behavior of the critical contacts when approaching the unjamming transition is approximately the same: ν increases up to a maximal value $\nu_c\simeq 8\%$ [27].

The loss of critical contacts occurring at the transition from loading to unloading in Fig. 3(b) also observed in [39], indicates that the *averaged* frictional state of the packing related to past solicitations is immediately modified. It is related to a systematic grain rearrangement, during which critical contacts leave the Coulomb frictional threshold. Note that the amount of critical contacts lost at the transition is not larger than the typical fluctuations around the averaged critical contact density ν during the cycle. In fact, the transition from loading to unloading imposed at θ_{rev} synchronizes the grain rearrangements for the various realizations, hence a larger response on average than in the other parts of the cycle. The effect of the reversal on a single realization remains an open issue, which is beyond the present averaged analysis.

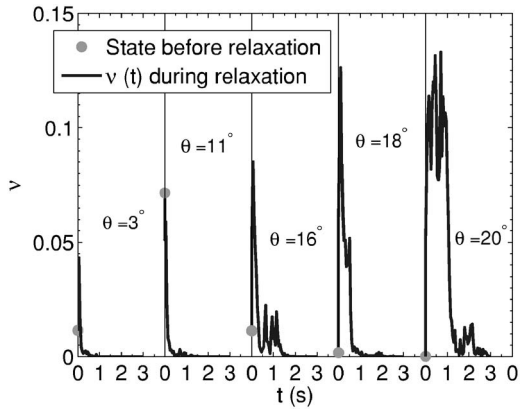

FIG. 4. Relaxation of the density of critical contacts ν as a function of time in five granular piles inclined at different angles ($\theta=3°,11°,16°,18°,20°$) after the rotation was stopped at $t=0$. The state of the pile just before the relaxation starts is represented by a circle.

We now observe the relaxation to a static packing in terms of critical contacts by suddenly stopping the rotation. Figure 4 shows the evolution of ν as a function of time after the rotation was stopped at $t=0$ in five granular piles inclined at different angles ($\theta=3°,11°,16°,18°,20°$). The state of the pile before the relaxation starts is represented by a circle. Whatever the density of critical contacts and the inclination when the packing start to relax, ν vanishes after a complex transient dynamics. The time needed for critical contacts to relax is larger for slopes close to θ_a: this confirms the complex relaxation towards equilibrium of a granular packing [12,22,23], and this is consistent with observations of long-range correlations close to the unjamming transition [22,27,30–32]. The relaxation of the critical contacts for rigorous static conditions shows that the critical state is a transient state. This can be understood by the fact that the contacts cannot sustain the sliding condition once the loading is stopped. In this sense, the density of critical contacts does not characterize the pile plastic state, because ν is a dynamic response function to the actual loading of the pile. Also other variables could be more representative of the plastic state of the pile—e.g., the averaged cumulative slip dislocation at critical contacts. However, critical contacts remain active during quasistatic loading, and it was shown that the evolution of ν for one realization [27] becomes more and more intermittent, exhibiting successive frictional demobilization and remobilization periods, when the rotation rate decreases.

Figure 5 shows the evolution of ν as a function of the pile slope during loading and unloading process for $\theta_{rev}=18°$. The density of critical contacts at an angle θ is smaller during unloading than during loading, as attested by the hysteretic loops. Figure 6 displays the evolution as a function of θ during the large cycles, of the correlation length r_c, defined as the mean size of clusters such that locally $\nu=\nu_c$. During each loading stage, r_c increases sharply above θ_r and is expected to reach the size of the pile at the unjamming transition, as shown in the case of monotonic external loading [27]. At the transition from loading to unloading, a signature of the loss of critical contacts is visible: r_c immediately reduces to a few grain diameters. There is no more evidence of correlation within the granular pile in terms of critical contacts upon reversal of the solicitation. Note that after the first loading, ν as well as r_c shows the same cyclic evolution, indicating the same behavior of critical contacts during the two successive cycles, especially when approaching the unjamming transition. The reduction of frictional mobilization after the reversal induces a strong hysteresis in both the evolution of ν and r_c during loading and unloading cycles. Is this hysteresis apparent on other global characteristics of the granular pile?

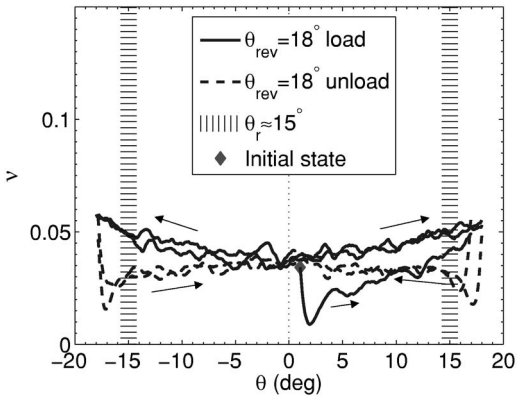

FIG. 5. Density of critical contacts ν averaged over 50 simulations, slide-averaged over 1° intervals as a function of the slope angle θ during the successive cyclic solicitations for $\theta_{rev}=18°$.

The critical contacts play a significant role when approaching the unjamming transition, since they likely give rise to microplastic events. Accordingly, one may wonder whether the response of the pile is modified by the hysteretic evolution of critical contacts observed in the range of slopes $[\theta_r;\theta_a]$. Also one would like to know whether the possible effect of the observed hysteresis is localized in the domain $[\theta_r;\theta_a]$ or conditions the response of the pile along the full cycle of solicitation. In the following, we investigate the hysteretic response of the pile to cyclic solicitations and the effect on this response of having approached the unjamming transition. To do so, we consider two different amplitudes of

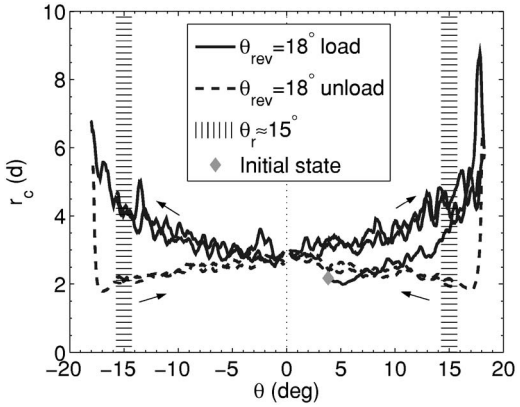

FIG. 6. Size of the correlated clusters of critical contacts r_c, slide-averaged over 1° intervals as a function of the slope angle θ during the successive cyclic solicitations for $\theta_{rev}=18°$.

loading-unloading cycles—namely, two values of the reversal angle θ_{rev}—and we compare the response of the granular pile in terms of stress, strain, and evolution of the contact network for $\theta_{rev}=10°$ and $\theta_{rev}=18°$.

IV. HYSTERETIC PHENOMENA DURING LOADING AND UNLOADING SOLICITATIONS

During cyclic tiltings, the induced stresses as well as the resulting deformations of the granular pile are investigated. We start with the comparison of the global stress state during loading and unloading stages.

A. Stress state of the granular pile

The maximal value of the shear to confinement ratio, the so-called inertial number in [13], is defined as $I_{max}=\gamma_{max}d\sqrt{\rho/P}$, with γ_{max} the maximal shear strain rate evaluated during coherent shearing in the range of slopes $[\theta_r;\theta_a]$, ρ the volumetric mass of the grains, and P the typical pressure induced by gravity. In the present case, $I_{max}\simeq 10^{-5}$ shows that the pile evolution is actually quasistatic. As a result, static stresses transmitted via contacts are much larger than kinematic ones due to momentum transport during collisions, so that the stress tensor of the granular pile $\boldsymbol{\sigma}$ in the xy frame is evaluated as follows from [42]:

$$\sigma_{ij}=\frac{1}{V}\sum_{\alpha=1}^{n^c} f_i^\alpha l_j^\alpha, \tag{1}$$

where i and j denote the space dimensions and α the contact. $\vec{f}$ is the contact force, $\vec{l}$ is the vector normal to the contact surface, and n^c is the total number of contacts in the representative element volume V. The tangential and normal stresses σ_T and σ_N along the direction of the free surface are calculated:

$$\sigma_N=\|(\boldsymbol{\sigma}\cdot\vec{n}_S)\cdot\vec{n}_S\|, \tag{2}$$

$$\sigma_T=\|\boldsymbol{\sigma}\cdot\vec{n}_S-\boldsymbol{\sigma}_N\cdot\vec{n}_S\|, \tag{3}$$

where $\vec{n}_S$ is the unity vector normal to the free surface. The direction of the eigenvector of $\boldsymbol{\sigma}$ corresponding to the largest eigenvalue is the principal stress direction, whose angle with the direction $\vec{n}_S$ is Ψ. The principal stress direction corresponds to the direction where stress is purely compressive.

Figure 7(a) displays the shear stress ratio σ_T/σ_N and Fig. 7(b) the evolution of the principal stress direction Ψ during small ($\theta_{rev}=10°$) and large ($\theta_{rev}=18°$) loading-unloading cycles. Both σ_T/σ_N and Ψ exhibit hysteretic evolutions related to irreversible modifications of the force transmissions at contacts, but the hysteresis loops are of rather small amplitude and independent of θ_{rev}.

During the first loading, $\sigma_T/\sigma_N\simeq a\tan(\theta)$ in agreement with the predictions of continuous-media mechanics for an infinite slope inclined in the gravity field at static equilibrium, except that a is not exactly equal to 1: $a=0.8$. It can be shown that this difference is to be attributed to finite-size and wall effects [32]. During the following cycles, σ_T/σ_N

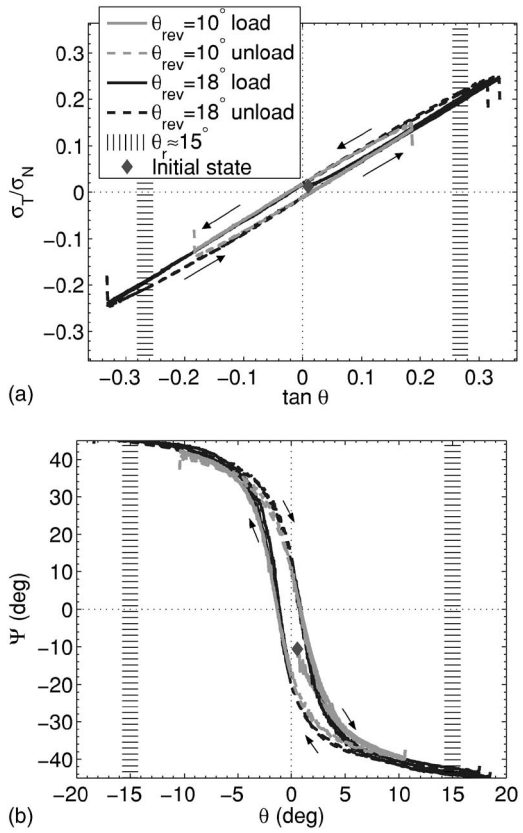

FIG. 7. Shear stress ratio σ_T/σ_N (a) and principal stress direction Ψ (b) as a function of the pile slope θ during cyclic rotations for small ($\theta_{rev}=10°$) and large ($\theta_{rev}=18°$) amplitudes. The vertical lines correspond to the value of $-\theta_r$ and θ_r. The initial state is represented by a diamond.

$\simeq a\tan(\theta)+\epsilon(\sigma_T/\sigma_N)_{res}$, where $\epsilon=-1$ ($\epsilon=+1$) during loading (unloading) and $a=0.8$. A residual stress ratio $(\sigma_T/\sigma_N)_{res}$ of the order of 5% of the typical shear stress ratio is recorded for $\theta\simeq 0°$. The principal stress direction Ψ tends to $\pm 45°$ for large inclinations, exhibiting a rather smooth evolution. For hydrostatic equilibrium—i.e., equal normal stresses $\sigma_{xx}=\sigma_{yy}$—it would be expected that $\Psi=-45°$ ($\Psi=+45°$) for $\theta>0$ ($\theta<0$).

The stress-state evolution of the granular pile is plotted in Fig. 7 for the two successive cycles: the plots perfectly collapse after the first loading. In the following, the two successive cycles are reported in all figures.

Altogether both the shear stress ratio σ_T/σ_N and the principal stress direction Ψ are controled by the inclination θ (and its temporal derivative, as evidenced by the weak hysteresis), whatever the solicitations path and the history of past cycles.

B. Deformation of the granular pile

The exploration of different metastable configurations results in the apparition of critical contacts in the packing, which induces local rearrangements of grains (see Sec. III and [27]). The effect of these rearrangements at the scale of the pile is apparent when plotting the variations of the volu-

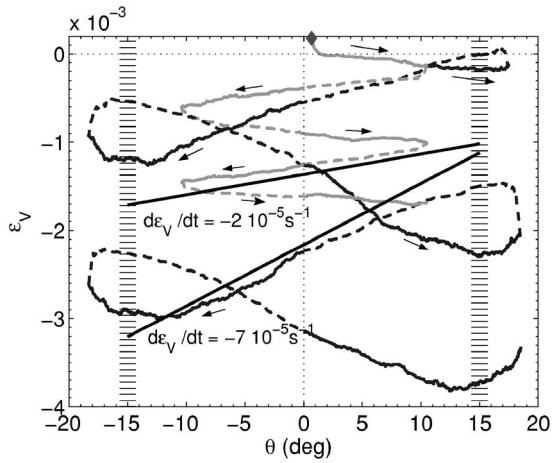

FIG. 8. Volumetric strain ϵ_V as a function of the pile slope during small and large cycles (same symbols as Fig. 7). The two lines are indications of the compaction rate $d\epsilon_V/dt$ for $\theta_{rev}=10°$ and $\theta_{rev}=18°$.

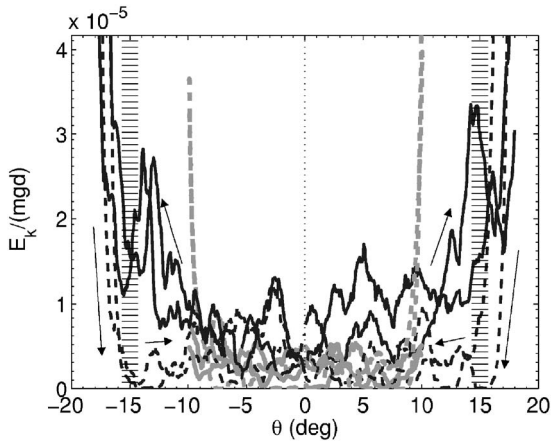

FIG. 9. Kinetic energy E_k averaged over all the grains and slide-averaged over 1° intervals, normalised by the typical potential energy of a grain of mass m for a height d, as a function of θ for $\theta_{rev}=10°$ and $\theta_{rev}=18°$ (same symbols as Fig. 7).

metric strain $\epsilon_V=(V-V_0)/V_0$, where V is the volume of the pile and V_0 its initial volume, as a function of the slope of the pile during successive small and large cycles (Fig. 8). At first sight, we notice that, even if the initial solid fraction C and the stress-state evolution of the pile are the same for the two cyclic amplitudes (Fig. 7), the volumetric strain evolution does depend strongly on θ_{rev}.

Irrespective of the value of θ_{rev}, cycles produce an overall densification of the pile of the order of 10^{-3}, corresponding to a slight increase of the solid fraction C from 0.785 to 0.79. Obviously, the small number of cycles experienced in the present work does not allow one to observe a saturation of the volume and eventually a critical state [9,43]. It is known that in similar cyclic solicitations [39], as well as in other experimental setups [10,44], even after a large number of cycles (10^4 cycles), the volume still slowly decreases.

For slopes $\theta \lesssim \theta_r$, the granular pile is contracting: ϵ_V decreases. On the contrary, for slopes in the range $[\theta_r;\theta_a]$, the rearrangements cause the granular pile to dilate: ϵ_V increases. As a result, for small cycles ($\theta_{rev}=10°$), the compaction of the granular pile remains monotonous (Fig. 8), whereas for large cycles ($\theta_{rev}=18°$), the granular pile exhibits compaction and dilation stages (Fig. 8). This latter behavior is typical when shearing dense granular media, because shear deformation is possible only if grains unjam, confirming the onset of a coherent shearing above θ_r.

Interestingly, the overall behavior of the pile over the complete solicitation is modified in the case of large cycles: the instantaneous compaction is twice more efficient for large cycles ($d\epsilon_V/dt \simeq -7\times10^{-5}$ s^{-1}) than for small ones ($d\epsilon_V/dt \simeq -2\times10^{-5}$ s^{-1}). As a result and despite the dilation stage occurring when $\theta \in [\theta_r;\theta_a]$, the overall densification is larger for large cycles than for small ones for the same number of cycles, showing that densification depends on the solicitation path [45]. This leads us to speculate that grains are much more allowed to rearrange when the pile has previously evolved in the coherent shear regime identified prior to the unjamming transition.

This largest susceptibility for grains to rearrange in the case of large cycles ($\theta_{rev}=18°$) is confirmed by monitoring the averaged kinetic energy of the grains E_k, represented as a function of the pile slope in Fig. 9 after slide-averaged over 1° intervals. The kinetic energy E_k involved in the local rearrangements, also occurring at small inclinations θ, is much higher when the granular pile has been loaded up above θ_r during its history. This evolution underlines the two different states and evolutions of the pile for the two cyclic amplitudes.

Exploring the domain $[\theta_r;\theta_a]$ allows for stronger rearrangements and larger volumetric strains during the full solicitation despite no apparent signature on σ_T/σ_N. As a result, the volumetric deformation of the granular pile shows a strong dependence on the amplitude of the cycles.

C. Evolution of the contact network

We now investigate the effect of the deformations on the evolution of the microstructure—i.e., the geometry of the contact network—which are candidates at relevant internal variables [8,9,46–50].

1. Coordinancy of the grains

The coordinancy Z—i.e., the mean number of contacts per grain, slide-averaged over 1° intervals—is plotted in Fig. 10 as a function of the pile slope during the cyclic solicitations. For both values of the amplitude θ_{rev}, the coordinancy Z varies less than 1%. Nevertheless, it exhibits a weak hysteresis according to the sense of rotation: Z tends to decrease during loading, but to increase during unloading.

Small and large cycles are identified by two different states: the value of the coordinancy depends on θ_{rev}. During small cycles ($\theta_{rev}=10°$), Z remains approximately at its initial value, by contrast with large cycles ($\theta_{rev}=18°$), for which a variation of the coordinancy occurs during the first exploration of the domain $[\theta_r;\theta_a]$ and remains afterwards.

The smallest coordinancy observed for $\theta_{rev}=18°$ corresponds to the densest granular piles, contrary to intuitive

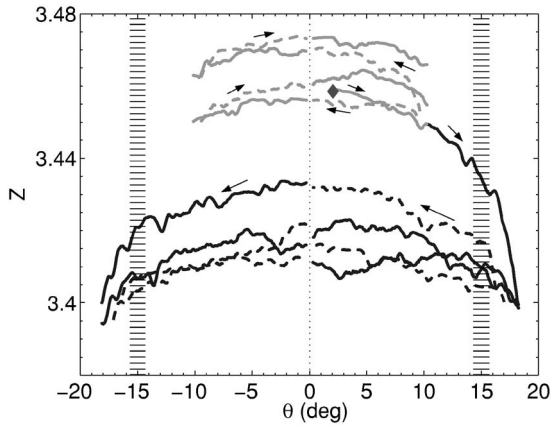

FIG. 10. Coordinancy of the grains Z slide-averaged over 1° intervals as a function of the slope of the pile for successive small and large cycles (same symbols as Fig. 7).

observations [51]. Such an anticorrelation between the evolutions of the coordinancy and volume under an external driving field could be related to the dependence of the packing equilibrium on its number of contacts. An "isostatic" packing has the minimal number of contacts required to remain at metastable equilibrium, by contrast with a "hyperstatic" one, which could lose some contacts and not its equilibrium. Yet for an initially static grain to rearrange, its contacts have to cooperate, which is easier for a smaller number of contacts. In the hyperstatic packing, a significant cooperation of contacts is needed for a grain to rearrange, by contrast with the isostatic packing, in which a slight change in the force transmission at contacts will enable a local rearrangement of grains. In the case of large cycles, the significant decrease of Z observed during the first loading makes the packing become less hyperstatic: grain rearrangements occur easily, enhancing the deformation of the pile.

2. Fabric of the pile

To further analyze the evolution of the microstructure of the pile, we now consider the statistics of the orientation of contacts. To do so, the fabric tensor $\boldsymbol{t}$ is computed using the following definition as defined in [52]:

$$t_{ij} = \frac{1}{n^c} \sum_{\alpha=1}^{n^c} n_i^\alpha n_j^\alpha, \tag{4}$$

where i and j denote the space dimensions and α the contact. $\vec{n}$ is the unity vector normal to the contact surface, and n^c is the total number of contacts. The fabric allows one to investigate the evolution of the geometry of the contact network, especially if contacts are created, opened, or modified such that their alignment tends towards a privileged direction. In particular, the anisotropic intensity Λ is calculated as

$$\Lambda = 2 \times (t_1 - t_2), \tag{5}$$

where t_1 and t_2 are, respectively, the larger and smaller eigenvalues of $\boldsymbol{t}$. In the case of an isotropic contact network—e.g., spatially periodical—the anisotropic intensity $\Lambda = 0$. The direction of the eigenvector of $\boldsymbol{t}$ corresponding to the largest eigenvalue is the fabric anisotropic direction, whose angle with the direction $\vec{n}_S$ is Φ.

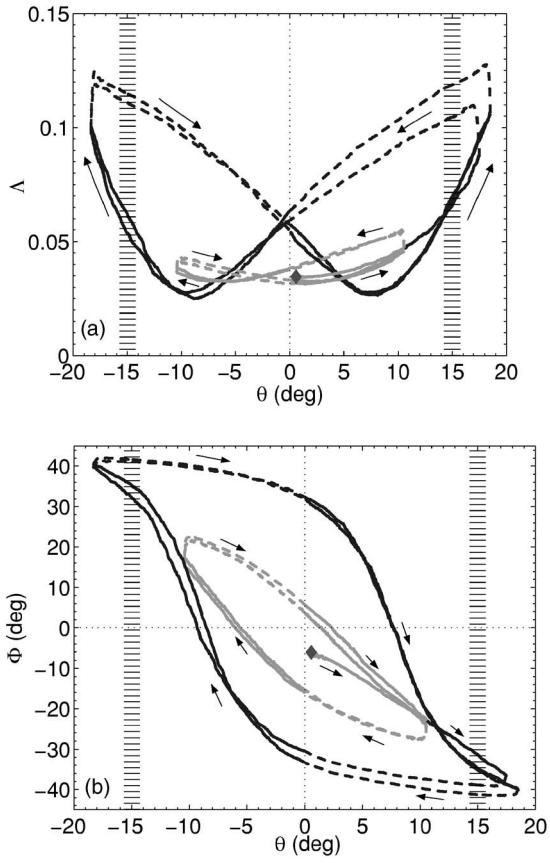

FIG. 11. Anisotropic intensity Λ (a) and fabric anisotropic direction Φ of the contact network (b) as a function of the pile slope during the successive cyclic rotations for $\theta_{rev} = 10°$ and $\theta_{rev} = 18°$ (same symbols as Fig. 7).

Figure 11(a) displays the evolution of the anisotropic intensity Λ as a function of the pile slope during the cyclic solicitations for $\theta_{rev} = 10°$ and $\theta_{rev} = 18°$. During small cycles, a rather isotropic state is observed, and only small variations of Λ with θ are observed ($\Lambda \simeq 0.05$): the geometry of the contact network is only weakly affected by the solicitation and remains close to the initial one. On the contrary, for large cycles, the anisotropic intensity evolves significantly, showing variations up to the maximum value $\Lambda \simeq 0.12$. Approaching the unjamming transition obviously strongly modifies the geometry of the contact network—e.g., by introducing structural anisotropy.

Figure 11(b) displays the evolution of the fabric anisotropic direction Φ as a function of the pile slope during the cyclic solicitations for $\theta_{rev} = 10°$ and $\theta_{rev} = 18°$. Irrespective of the value of θ_{rev}, Φ evolves during the solicitations and rotates in the sense opposite to the driving rotation: Φ decreases (increases) when θ increases (decreases). Following this evolution, the fabric anisotropic direction tends to approach that of the free surface, and for large inclinations, Φ tends towards the principal stress direction $\Psi = \pm 45°$. This behavior corresponds to the mechanisms of creation of contacts in the direction of compressive stress and the loss of contacts in the direction of extension.

Besides these general observations, the contact network evolution exhibits more complex features. Both for small and large cycles, the fabric exhibits a strongly marked hysteresis, probing the irreversible modifications of the disordered microstructure. The hysteresis loops of Λ and Φ are very smooth. Furthermore, when the granular pile has approached the unjamming transition—namely, for large cycles ($\theta_{rev}=18°$)—the shape of the hysteresis is dramatically changed and the loop amplified. This points out the peculiar effect of coherent shearing occurring prior to the unjamming transition on the granular packing evolution. More particularly, the fabric evolves less rapidly during unloading than during loading for large cycles ($\theta_{rev}=18°$). In other words, the packing seems to be less able to reorganize its structure during unloading than during loading when having approached the unjamming transition in its history. The same remark applies both to the evolution of the anisotropic intensity Λ and to the fabric anisotropic direction Φ. This may be rather unexpected given that the efficiency of rearrangements is increased in the case of large cycles and this during the complete solicitation.

Note that for large amplitudes ($\theta_{rev}=18°$), the hysteretic cycles of Λ and Φ are symmetric, by contrast with small amplitudes ($\theta_{rev}=10°$), for which an asymmetry related to the initial fabric anisotropy remains. Exploring the range of slopes $[\theta_r;\theta_a]$ when approaching the unjamming transition allows a profound modification of the contact network according to its initial state, by increasing structural disorder.

Altogether the fabric of the pile (Z, Λ, and Φ) at an angle θ strongly depends on the solicitation path, as observed for the pile deformation (ϵ_V and E_k).

V. RESPECTIVE ROLE OF STRONG AND WEAK CONTACTS

Dense quasistatic granular media are known to exhibit two complementary contact networks, strong and weak, depending on the intensity of the normal force transmitted at contacts [32,34,35,53,54]. Very recently, the role of the critical contacts in the destabilization of a pile [27,33], as well as in the elastoplastic response of a granular packing [46] has also been underlined. Still, it was shown that during the slow tilting under gravity of a granular pile, critical contacts and more generally high frictional contacts are mainly weak contacts [27,33]. Here, in the line of these studies [32,34,35,53,54] and as a first step towards the understanding of the role of the microstructure and the heterogeneous nature of contacts in the observed hysteresis, we choose to concentrate on the respective contributions of the strong and weak contacts to the hysteretic behavior of the pile. Further works should definitely examine in more detail the role of highly frictional contacts in the spirit of [33,46].

Accordingly, the computation of the stress and fabric tensors is now restricted to strong or weak contacts using, respectively, Eq. (1) and (4). In the present work, since a vertical gradient of the contact forces is related to the gravity field, a contact at a depth y is defined as strong (weak) if it transmits a normal force larger (smaller) than the averaged normal forces at depth y.

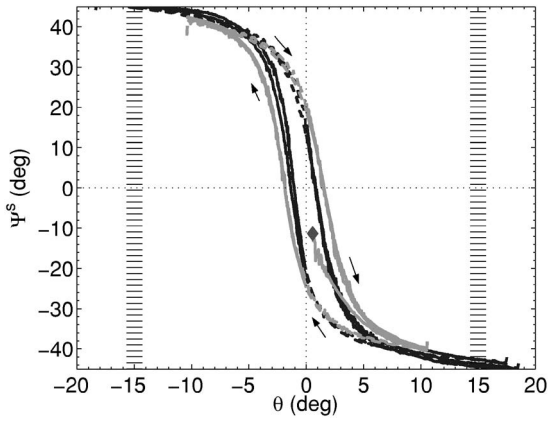

FIG. 12. Principal stress direction in the strong contact network Ψ^s as a function of the pile slope during the successive loading-unloading cycles for small and large amplitudes (same symbols as Fig. 7).

A. Strong-contact network

Figure 12 displays the principal stress direction in the strong-contact network Ψ^s as a function of the surface slope during small ($\theta_{rev}=10°$) and large ($\theta_{rev}=18°$) cycles. The evolution of Ψ^s is weakly hysteretic as a function of the pile slope, and the hysteresis is approximately the same irrespective of the amplitude of the solicitation, as observed previously for the total contact network [Fig. 7(b)]. The strong-contact network represents by far the largest contribution to the global stress [34]. Accordingly Ψ^s and Ψ exhibit very similar behaviors.

The fabric anisotropic direction of the strong contact network Φ^s is displayed as a function of the pile slope during the cyclic solicitations in Fig. 13. The evolution of Φ^s exhibits hysteresis during the cycles of both amplitudes. However, unlike the previous observations on the fabric of the total contact network [Fig. 11(b)], the size of the hysteresis loops is small for $\theta_{rev}=10°$ and 18°. The evolution of Φ^s is very much correlated with the evolution of Ψ^s, and the shapes of the hysteresis loops of both Ψ^s and Φ^s are smooth.

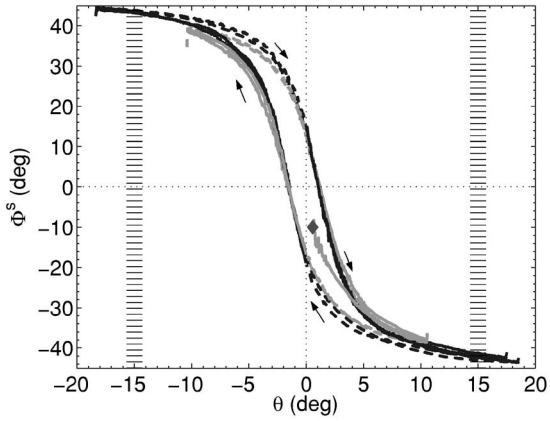

FIG. 13. Fabric anisotropic direction of the strong contact network Φ^s as a function of the pile slope during successive loading-unloading cycles for small and large amplitudes (same symbols as Fig. 7).

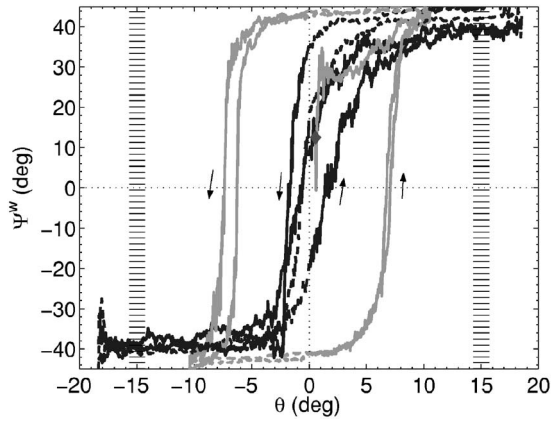

FIG. 14. Principal stress direction in the weak-contact network Ψ^w as a function of the pile slope during the cycles for small and large amplitudes (same symbols as Fig. 7).

During cyclic solicitations, neither the stress nor the fabric of the strong-contact network is sensitive to the amplitude of the cycles.

B. Weak-contact network

Figure 14 displays the principal stress direction in the weak-contact network Ψ^w as a function of the surface slope during small ($\theta_{rev}=10°$) and large ($\theta_{rev}=18°$) cycles. The evolution of Ψ^w is strongly influenced by the amplitude of the solicitations. This qualitative change is not reflected by the total-contact network response [Fig. 7(b)] due to the dominant contribution of the strong-contact network to the global stress [34].

Figure 15 displays the evolution of the fabric anisotropic direction of the weak-contact network Φ^w as a function of the pile slope for small ($\theta_{rev}=10°$) and large ($\theta_{rev}=18°$) cycles. The response of the weak-contact network is again strongly dependent on the cycles amplitude θ_{rev}, by contrast with the response of the strong-contact network (Fig. 13). For small cycles ($\theta_{rev}=10°$), Φ^w exhibits nearly no hysteresis and remains approximately always normal to Φ^s, as observed in the case of continuous loading [33]. On the contrary, for large cycles ($\theta_{rev}=18°$), a strong hysteretic behavior is observed, which consists of a premature rotation of Φ^w upon reversal: Φ^w switches beforehand during unloading in comparison with loading. This effect leads to a remarkable orientation of the fabric of the two contact networks: Φ^w and Φ^s are equal during a part of the cycle, attesting to the temporary alignment of the privileged direction of the two contact networks. The particularly early evolution of the weak-contact network geometry when the pile has approached the unjamming transition is actually responsible for the delay observed in the reorganization of the total-contact network. As a consequence, upon reversal, the packing keeps the memory of the previous orientation of the total-contact network during a large part of the cycle [Fig. 11(b)].

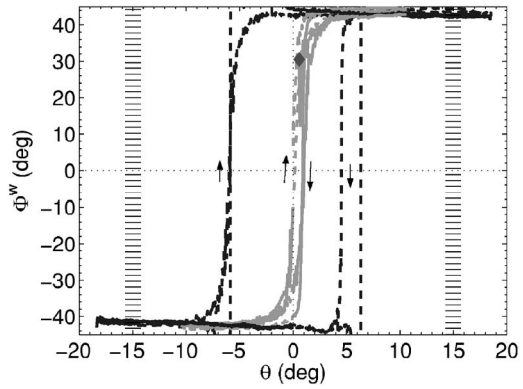

FIG. 15. Fabric anisotropic direction of the weak-contact network Φ^w as a function of the pile slope θ during small and large cycles (same symbols as Fig. 7).

Contrary to the smooth shape of the hysteresis loops in the strong-contact network (Fig. 13) and in the total-contact network [Fig. 11(b)], the hysteresis loops in the weak-contact network (Fig. 15) exhibit an abrupt macroscopic jump. It should also be mentioned that the weak-contact network response exhibits large fluctuations from one realization to another one. These fluctuations are strongly enhanced close to the unjamming transition. Evidence of these fluctuations is, for instance, the noisy signal for Ψ^w (Fig. 14) and the absence of superposition of the hysteretic loops for Φ^w (Fig. 15).

Altogether, in the weak-contact network by contrast with the strong one, both stress and fabric are very sensitive to the amplitude of the cyclic solicitations. Two conclusions can be drawn from these observations.

(i) In the limit of small solicitations—e.g., for cycles with $\theta_{rev}=10°$—the hysteretic behavior of the granular pile when looking at both the stress and fabric states is dominated by the strong-contact network contribution.

(ii) For large cycles, with $\theta_{rev}>\theta_r$—namely, when the pile approaches the unjamming transition—the response of the weak-contact network becomes strongly affected and the hysteretic behavior of the pile is strongly modified despite the lack of modification of the response of the strong-contact network.

Accordingly the hysteretic behavior of the pile is the result of a complex interplay between the strong- and weak-contact networks, whose relative contributions strongly depend on the amplitude of the cycles.

VI. DISCUSSION AND CONCLUSION

The successive tiltings of the granular pile from different initial conditions up towards the avalanche angle allow one to demonstrate that the density and correlation length of the critical contacts are relevant dynamic response functions to describe the metastable evolution of the packing towards the unjamming transition under external loading. Due to the transient nature of the critical contact state, these quantities are representative of actual loading of the pile, but they do not characterize its plastic state.

The response of the granular packing to the quasistatic cyclic solicitations reveals that the evolution of the critical contacts is hysteretic when the pile has approached the un-

jamming transition. At the transition from loading to unloading, critical contacts cannot anymore sustain the sliding condition, so that the frictional state of the packing is immediately removed, attesting to the end of coherent shearing, as observed in the case of experimental shear reversal [23,37].

When looking for such memory effects on other features of the pile—namely, on stress, strain, and fabric—they exhibit different responses. The stress state exhibits weak hysteretic evolutions as a function of the slope, and the hysteresis is revealed to be independent of the amplitude of the cycles. On the contrary, the strain and fabric evolutions of the pile, related to structural disorder, are very sensitive to the amplitude of the cycles. These observations will hardly be explained by a simple constitutive law relating only stress and strain of the granular pile: such a relation should be not so trivial, but should take into account the anisotropy of the pile microstructure [46–50,55]. The observation of piles with the same stress state, but characterized by different granular fabrics, would suggest that stress induced by gravity is transmitted in the pile whatever the geometry of the total contact network and whatever the structural disorder level.

Further analyses of the strong- and weak-contact contributions to the macroscopic behavior allow us to clarify these intriguing observations. In the strong-contact network, neither the stress nor the fabric depends on the solicitation amplitude. In the weak-contact network, both the stress and the fabric are sensitive to the cyclic amplitude. The apparent mismatch between stress and fabric at the scale of the total contact network does not survive when separating weak- and strong-contact network contributions. It simply comes from the strong-contact network weight in the overall stress [34]. Accordingly, the above analyses stress the relevance of a constitutive law which specifies the two-phase nature—weak and strong—of granular media. In the strong-contact network, stress and fabric are very much synchronized and a rather simple relation could relate them. The behavior of the weak-contact network is much more complex. A strong memory of the unjamming transition affects the response of the weak-contact network during the full solicitation, probably due to high sensibility of weak contacts to coherent shearing occurring prior to the unjamming transition. Finally the observed fluctuations in the weak-contact network are presumably related to long-range correlations. These correlations within the pile allow a local rearrangement of grains to further propagate and to affect essentially the weak contacts, due to their highest frictional mobilization, as recently shown in [27,33]. This high sensibility of the weak contacts to local perturbations enables them to evolve collectively and to change the microstructure of the packing. A signature of the localization of the correlations in the weak-contact network could be seen in the particular shape of the hysteresis loops. Whereas the loops are very smooth in the total and strong contact networks, the hysteresis loops in the weak contact network exhibit abrupt macroscopic jumps. These respective delay and instantaneous responses could be related to the relative contribution of structural disorder and finite-size interactions or correlations, as suggested in [56,57]. In this picture, the hysteresis with a jump in the weak-contact network would suggest that the size of correlations is larger than the typical length scale of the structural disorder in this phase, contrary to the predominant role of disorder in the microstructure of the packing. Altogether, such complex behaviors—spatial correlations and memory effects—call for more elaborated constitutive laws as in [46–50,55].

To conclude, the behavior of the pile is strongly modified close to the unjamming transition, as experimentally observed [22,28,31], coinciding with important irreversible modifications of the microstructure. These modifications result from a specific solicitation of weak contacts: these latter play a considerable role in the behavior of the pile despite their marginal contribution to the stress state. The present paper demonstrates the relevance of a two-phase description, not only for the destabilization process, but also for the quasistatic rheology, as soon as the granular sample has approached the unjamming transition in its past history. Further studies should investigate the complex behavior of the weak phase in order to extract a constitutive relation for granular materials, accounting for their two-phase nature.

ACKNOWLEDGMENTS

We wish to thank the French Groupe de Recherche Milieux Divisés and, more especially J. H. Snoeijer, P. Claudin, J.-N. Roux, and E. Kolb for their discussions on the present work. L.S. acknowledges Marie Curie European Grant No. 500511 for financial support.

[1] P. Sollich, F. Lequeux, P. Hebraud, and M. E. Cates, Phys. Rev. Lett. **78**, 2020 (1997).

[2] J.-N. Roux, Phys. Rev. E **61**, 6802 (2000).

[3] H. Troadec, F. Radjai, S. Roux, and J. C. Charmet, Phys. Rev. E **66**, 041305 (2002).

[4] H. M. Jaeger, S. R. Nagel, and R. P. Behringer, Rev. Mod. Phys. **68**, 1259 (1996).

[5] M. Oda and K. Iwashita, *Mechanics of Granular Materials: An Introduction* (Balkema, Rotterdam, 1999).

[6] P. G. de Gennes, Rev. Mod. Phys. **71**, S374 (1999).

[7] J. Rajchenbach, Adv. Phys. **49**, 229 (2000).

[8] S. Nemat-Nasser and M. Hori, *Micromechanics: Overall properties of heterogeneous solids*, 2nd ed. (Elsevier, Amsterdam, 1999).

[9] F. Radjai and S. Roux, in *The Physics of Granular Media* edited by H. Hinrichsen and D. E. Wolf (Wiley, Berlin, 2004).

[10] J. B. Knight, C. G. Fandrich, C. N. Lau, H. M. Jaeger, and S. Nagel, Phys. Rev. E **51**, 3957 (1995).

[11] C. S. O'Hern, S. A. Langer, J. A. Liu, and S. R. Nagel, Phys. Rev. Lett. **86**, 111 (2001).

[12] R. R. Hartley and R. P. Behringer, Nature (London) **421**, 928 (2003).

[13] G. D. R. MiDi, Eur. Phys. J. E **14**, 341 (2004).
[14] A. J. Liu and S. R. Nagel, Nature (London) **396**, 21 (1998).
[15] C. S. O'Hern, L. E. Silbert, A. J. Liu, and S. R. Nagel, Phys. Rev. E **68**, 011306 (2003).
[16] L. Berthier, L. F. Cugliandolo, and J. L. Iguain, Phys. Rev. E **63**, 051302 (2001).
[17] O. Pouliquen, M. Belzons, and M. Nicolas, Phys. Rev. Lett. **91**, 014301 (2003).
[18] A. Coniglio, A. Fierro, H. J. Herrmann, and M. Nicodemi, *Unifying Concepts in Granular Media and Glasses* (Elsevier, Amsterdam, 2004).
[19] G. Marty and O. Dauchot, Phys. Rev. Lett. **94**, 015701 (2005).
[20] S. F. Edwards, *Granular Matter: An Interdisciplinary Approach* (Springer, New York, 1994).
[21] I. K. Ono, C. S. O'Hern, D. J. Durian, S. A. Langer, A. J. Liu, and S. R. Nagel, Phys. Rev. Lett. **89**, 095703 (2002).
[22] S. Deboeuf, E. M. Bertin, E. Lajeunesse, and O. Dauchot, Eur. Phys. J. B **36**, 105 (2003).
[23] B. Utter and R. P. Behringer, Eur. Phys. J. E **14**, 373 (2004).
[24] A. Mehta and G. C. Barker, Europhys. Lett. **56**, 5 (2001).
[25] G. Metcalfe, S. G. K. Tennakoon, L. Kondic, D. G. Schaeffer, and R. P. Behringer, Phys. Rev. E **65**, 031302 (2002).
[26] K. E. Daniels and R. P. Behringer, Phys. Rev. Lett. **94**, 168001 (2005).
[27] L. Staron, J.-P. Vilotte, and F. Radjai, Phys. Rev. Lett. **89**, 204302 (2002).
[28] A. Kabla, G. Debregeas, J.-M. di Meglio, and T. J. Senden, Europhys. Lett. **71**, 10165 (2005).
[29] L. E. Silbert, A. J. Liu, and S. R. Nagel, Phys. Rev. Lett. **95**, 098301 (2005).
[30] H. M. Jaeger, C. Liu, and S. R. Nagel, Phys. Rev. Lett. **62**, 40 (1989).
[31] A. Daerr and S. Douady, Nature (London) **399**, 241 (1999).
[32] L. Staron, J.-P. Vilotte, and F. Radjai, Eur. Phys. J.(to be published).
[33] L. Staron and F. Radjai, Phys. Rev. E **72**, 041308 (2005).
[34] F. Radjai, D. E. Wolf, M. Jean, and J.-J. Moreau, Phys. Rev. Lett. **80**, 61 (1998).
[35] F. Radjai, M. Jean, J. J. Moreau, and S. Roux, Phys. Rev. Lett. **77**, 274 (1996).
[36] S. Nasuno, A. Kudrolli, and J. P. Gollub, Phys. Rev. Lett. **79**, 949 (1997).
[37] M. Toiya, J. Stambaugh, and W. Losert, Phys. Rev. Lett. **93**, 088001 (2004).
[38] N. W. Mueggenburg, Phys. Rev. E **71**, 031301 (2005).
[39] F. Alonso-Marroquín and H. J. Herrmann, Phys. Rev. Lett. **92**, 054301 (2004).
[40] R. García-Rojo, F. Alonso-Marroquín, and H. J. Herrmann, e-print cond-mat/0505507, Phys. Rev. E (to be published).
[41] M. Jean and J.-J. Moreau, in Proceedings of Contact Mechanics International Symposium (Presses Polytechniques et Universitares Romandes, Lausanne, Switzerland, 1992), pp. 31–48.
[42] N. P. Kruyt and L. Rothenburg, J. Appl. Mech. **706**, 118 (1996).
[43] P. Evesque, D. Fargeix, P. Habib, M. P. Luong, and P. Porion, Phys. Rev. E **47**, 2326 (1993).
[44] M. Nicolas, P. Duru, and O. Pouliquen, Eur. Phys. J. E **3**, 309 (2000).
[45] H. A. Joer, J. Lanier, and M. Fahey, Geotechnique **48**, 5 (1998).
[46] F. Alonso-Marroquín, S. Luding, H. J. Herrmann, and I. Vardoulakis, Phys. Rev. E **71**, 051304 (2005).
[47] M. Madadi, O. Tsoungui, M. Ltzel, and S. Luding, Int. J. Solids Struct. **41**, 2563 (2004).
[48] C. Thornton and D. J. Barnes, Acta Mech. **64**, 45 (1986).
[49] R. J. Bathurst and L. Rothenburg, J. Appl. Mech. **55**, 17 (1988).
[50] S. Nemat-Nasser, J. Mech. Phys. Solids **28**, 1561 (2000).
[51] L. E. Silbert, D. Ertas, G. S. Grest, T. C. Halsey, and D. Levine, Phys. Rev. E **65**, 031304 (2002).
[52] M. Satake, *Deformation and Failure of Granular Materials* (Balkema, Rotterdam, 1982).
[53] S. J. Antony, Phys. Rev. E **63**, 011302 (2000).
[54] E. Aharonov and D. Sparks, Phys. Rev. E **65**, 051302 (2002).
[55] I. Vardoulakis, Ing.-Arch. **59**, 106 (1989).
[56] K. Dahmen and J. P. Sethna, Phys. Rev. B **53**, 14872 (1996).
[57] Y. Jiang, P. J. Swart, A. Saxena, M. Asipauskas, and J. A. Glazier, Phys. Rev. E **59**, 5819 (1999).